32ND INTERNATIONAL COSMIC RAY CONFERENCE, BEIJING 2011

Design & Performance of LHAASO-WCDA Experiment

ZHIGUO YAO[1], HANRONG WU[1], MINGJUN CHEN[1], BO GAO[1] AND BIN ZHOU[1] FOR THE LHAASO COLLABORATION
[1]*Institute of High Energy Physics, Beijing, 100049, China*
zhiguo.yao@ihep.ac.cn
DOI: 10.7529/ICRC2011/V09/0772

Abstract: As one of major components of the LHAASO Project, A Water Cherenkov Detector Array (WCDA) of size about 80000 m^2 is to be built in Yang-Ba-Jing, Tibet, China. The main physics target of it is to survey the sky for Gamma ray sources at the energy range 100 GeV – 30 TeV. Technical design details, including the configuration of the array, the setup of calibration systems, the specification of electronics and DAQ system, are briefly introduced; the performance of the array on several aspects of Gamma astronomy, especially on surveying extragalactic flares, are studied and reported.

Keywords: LHAASO, WCDA, Gamma astronomy, all sky survey.

1 Introduction

The Very-high-energy (VHE, >100 GeV) gamma ray is a great messenger to probe the most energetic accelerators in the Universe, as it can travel in a straight line from the source to the observer on the Earth. A new window on astrophysics study is opened from the first clearly detection of the VHE gamma ray source – the Crab Nebula, in 1989 [1], with the imaging atmospheric Cherenkov technique. So far more than 100 VHE gamma ray sources have been detected [2], and the high energy sky has revealed a stunning richness of new phenomena and puzzling details [3].

Surveying the sky for more sources with high sensivity and monitoring their emission intensity at VHE energies are very important for understanding the evolution of galaxies (such as AGN) and the acceleration mechanisms in gamma ray sources. Complementary to the Cherenkov telescopes, ground-based particle detector arrays, due their high duty cycle ($> 95\%$) and large field of view ($> 2\pi/3$), allow to play an important role on these physics studies. The Water Cherenkov Detector Array (WCDA) of the Large High Altitude Air Shower Array (LHAASO) project [4] is planned to be built in Yang-Ba-Jing (YBJ, 4300 m a.s.l.), Tibet, China, aiming to give a sensitive explore to the VHE sky.

In this paper, the technical design details of the LHAASO-WCDA, including the configuration of the array, the water purifier and recirculation system, the setup of calibration systems, the requirement to electronics and DAQ systems, are briefly introduced in section 2; the performance of the array on several aspects of Gamma astronomy, especially on surveying extragalactic flares, are studied and reported in section 3.

2 Detector design

2.1 Detector configuration

The projected LHAASO-WCDA consists of 4 water ponds, octagonal in shape for each, inscribed to a square with size $150 \times 150\ \mathrm{m}^2$. The depth of the pond is about $4.5\ m$. Each pond is subdivided into $30 \times 30 = 900$ cells sized $5 \times 5\ \mathrm{m}^2$, partitioned by black plastic curtains to prevent the crosstalk of lights yielded in neighboring cells. A 8” hemispheric PMT resides in the bottom of each cell, looking upward to collect Cherenkov lights produced by charged particles in the air shower secondaries, recording the time and the charge information. Every 3×3 cells forms a *group*, and 4 neighboring groups makes up a *cluster*, as shown in figure 1.

For better discriminating gamma and proton showers, a layer of muon detectors is planned to be built in the bottom of the pond. A preliminary design (figure 2) is to increase the water depth to 6 m, using the bottom 1.5 m depth for muons. This muon layer is curtained by reflective Tyvek films, deployed with 10” PMTs upside down for every $10 \times 10\ \mathrm{m}^2$ area to collect lights generated by passing though muons. The water depth, 4 m above the muon layer is anticipated to absorb most of the electro-magnetic components among the shower secondaries.

The pond is to be covered under a roof made of color plates. A thick layer of black HDPE plastics film is paved beneath the roof; and a layer of shading cover made of fabric and cloth is laid 50 cm above the water surface. These measures fulfill the requirement of the light tightness of the pond.

Depending on the engineering issues and the sensitivity optimization, there is also a possibility to merge these 4 ponds

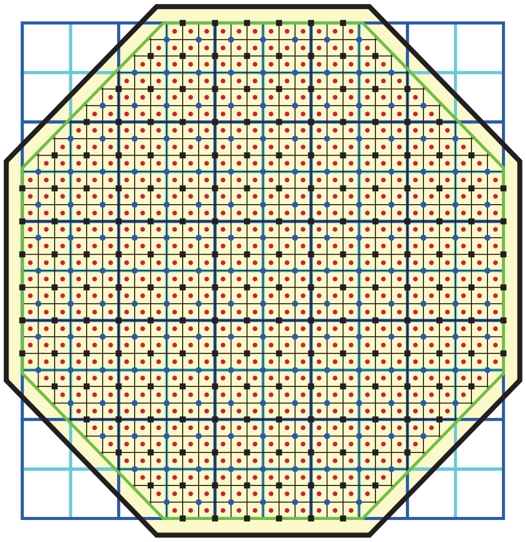

Figure 1: Schematic layout of one of the pond of the LHAASO-WCDA project, whose area is about $18,640\ \mathrm{m}^2$, consisting of 21 clusters, deployed with 720 PMTs.

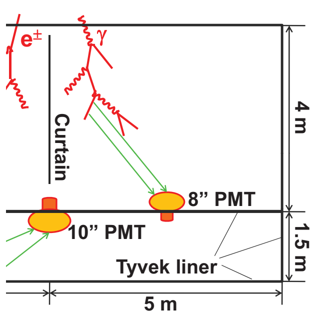

Figure 2: Schematic profile of the pond of the LHAASO-WCDA project. The water depth above the 8” PMT is 4 m. A very preliminary design of the muon detectors in the bottom layer is also drawn.

into a big octagonal one with total area of $75,000\ \mathrm{m}^2$, inscribed to a rectangle of size $300 \times 300\ \mathrm{m}^2$.

2.2 Water purifier and recirculation system

It is always essential for water Cherenkov detectors to keep the cleanness of water for the whole operating period. A water purifier and recirculation system is designed for this purpose. The water purifier (figure 3) are made up of the following components: a multimedia filter, an activated carbon filter, two fine filters ($5\ \mathrm{upmum}$ and $1\ \mathrm{upmum}$), an ultra-fine filter ($0.22\ \mathrm{upmum}$), and UV lamps ($254\ \mathrm{ns}$ and $185\ \mathrm{ns}$). The UV lamp at $185\ \mathrm{ns}$ is especially important for the system because it can destroy the dissolved total organic carbon which is believed to the main source of the pollution in the water. The water purified by this system can easily reach the transparency (attenuation length) above 20 m for lights at around 400 nm wavelength, fulfilling the requirement of the experiment.

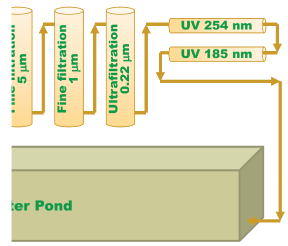

Figure 3: Schematic drawing of water purifier setup.

Water from a well is supplied to the purifier, and then poured by pumps into the pond through a pipe net distributed at the bottom of the pond. Many small holes are punched along these pipes, allowing a uniform injection of the water. Another similar set of pipe net is installed on the top of the pond, about 30 cm below the water surface, starting to continuously draw the pond water to the purifier after the pond has been filled. See figure 4 for the schematic of the pipe nets. The pump and the purifier works all along in a fixed flow rate that can recirculate the whole pond water through the pipe nets in about 1 month.

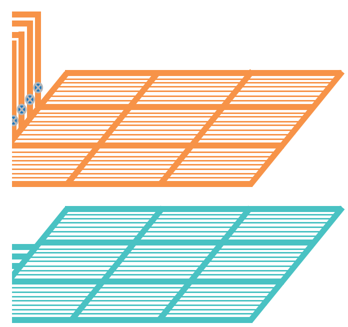

Figure 4: Schematic drawing of the water recirculation system.

2.3 Calibration systems

Two sets of calibration systems, on time and charge respectively, are tentatively designed for the LHAASO-WCDA.

The time calibration is realized by an optical fiber system [5]. On side top of every PMT, two optical fibers with approximately 20 m difference in length are connected. All the fibers in a cluster are bundled together, illuminated by a uniform light source consists of a array of LEDs. These LEDs are powered by a same circuit which can guarantee a fast rise-time ($< 10\ \mathrm{ns}$) of the LED light pulse output. For every cluster, at least two short fibers are exchanged with two neighboring clusters, enabling a cross calibration of clusters. LEDs are pulsed in a rate of 10 Hz, automatically triggering the DAQ system, so that there is enough statistics to calibrate the whole pond in a time scale of 1 hour, while the data-taking for air showers keeps continuously running. With an proper selection and design of the fibers, LEDs, the drivers, and the cross calibration method, all the PMTs in the pond can achieve a precision < 0.2 ns for the time offset measurement.

The charge of the PMT signals is calibrated in two ranges: the single photo-electron (SPE) spectrum of the counting rate and the signal of nearly vertical muons hitting the PMT cathode. For the former, attributed to the high single rate of PMT in water, it is possible to fit the charge distribution, which is peaked at the SPE position [6], so that the gain of each PMT is got. For the latter, thanks to the enhancement of the number of photo-electrons (PEs) for muons [6] hitting on the cathode, the peak position of these signals can be distinctly revealed by placing a shade pad of size $\sim 1 \times 1\ \mathrm{m}^2$ on 15 cm above the PMT top [7]. This method can calibrate the PMT charge in a precision of a few percent, involving all the effects, such as the quantum efficiency, the geometrical effect, the collection efficiency, and the electronics.

2.4 Trigger and electronics requirement

The counting rate of the PMT in the pond is estimated to be around 50 kHz, caused by the cosmic ray secondaries, bringing a big challenge to the electronics. A two-tier trigger pattern catering to shower features is tentatively designed to avoid the influence of the single channel noises. The first is the group trigger: any 3 PMTs in a group are fired within any 100 ns duration, the group is triggered; the number of fired PMTs in the group is named the *group multiplicity*. The next is the master trigger: the group triggers are processed, and the array is then triggered once when one of the following combinations of group triggers is satisfied in a duration of 700 ns: a) 1(M9); b) 1(M7) + 1(M3); c) 1(M6) + 1(M4); d) 2(M5); e) 1(M5) + 2(M3); f) 3(M4) + 1(M3); g) 2(M4) + 3(M3); h) 6(M3); where y(Mx) means that *at least* y groups have the group multiplicity x.

The number of photo-electron (nPE) distribution for each PMT, obtained from a simulation of gammas from Crab nebula, is mainly concentrated at 1 PE (43%) and 2 PEs (18%); the chance for a big nPE is much rare, e.g., $< 2 \cdot 10^{-4}$ for $\mathrm{nPE} > 2000$. It is rare too even for high energy gammas ($E > 5$ TeV), the chance is $7 \cdot 10^{-4}$ for $\mathrm{nPE} > 2000$, see figure 5. A simulation shows that a saturation of the charge measurement at 4000 PEs has marginal effect to the sensitivity of the detector.

For a PMT, the arrival time of Cherenkov lights generated by a shower is very short, depending mainly on the depth of shower front. Simulations show that the pulse width (0–90% PEs) for 90% PMTs is smaller than 13 ns, see figure 6. The pulse width turns wider for slant showers, but is still smaller than 18 ns.

In a simulation, a jitter of 1 ns is added to smear the arrival time of the PMT, but no obvious sensitivity degradation is found.

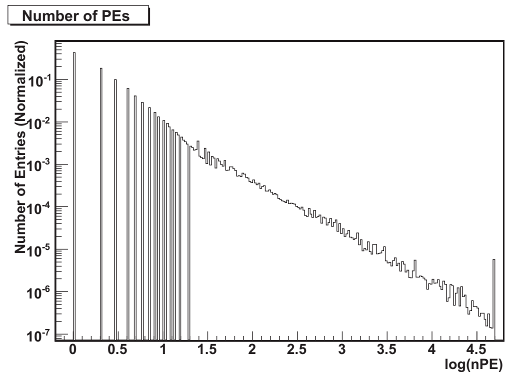

Figure 5: nPE distribution for each PMT, obtained from a simulation of gammas from Crab nebula.

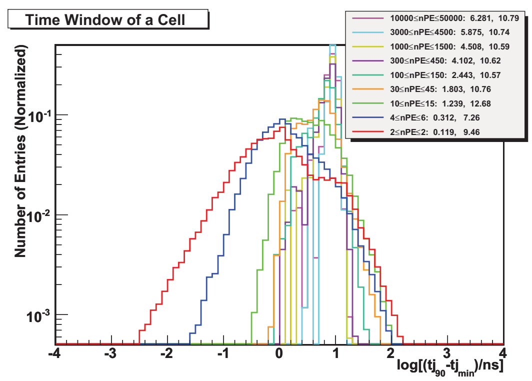

Figure 6: The simulated distribution of pulse width (0–90% PEs) for any a PMT in detecting air showers.

The trigger rate of a pond is around 15 kHz. The details can be found in [8].

3 Sensitivity

The sensitivity of the LHAASO-WCDA has been estimated based on a full Monte Carlo simulation, see [8] for the details of the procedure. The sensitivity of all the 4 independent ponds is given in figure 7, compared to the curves of other ongoing or projected experiments. In the plot, One year's operation time for wide field of view (WFOV) detectors (e.g., particle detector array) is used, contrasting to 50 hours' observation time of Cherenkov telescopes. This kind of duration selection is usually for the observation of known stable sources.

As to a flaring outburst of a source, IACTs usually have no chance to detect or observe it, unless receiving an alert from other experiments. Even there is a timely alert, IACTs still have big probability to miss it because of their limited duty cycle, i.e. the influence of Sun, Moon and weather conditions. Assuming a flare lasting for 3 days appeared in the Crab transit, the sensitivity of LHAASO-WCDA can

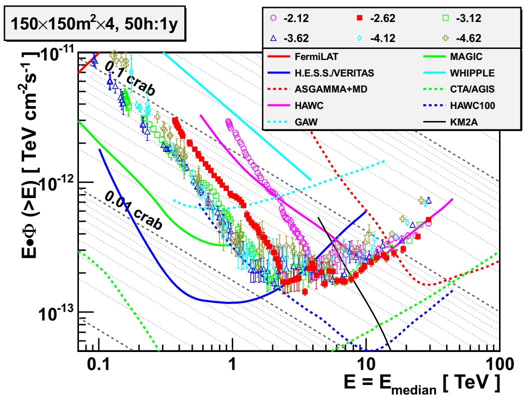

Figure 7: Sensitivity of LHAASO-WCDA configured in 4 independent ponds. The curves for other experiments are drawn for a comparison. The observation time is 1 y and 50 h for WFOV detectors and IACT respectively.

reach to a level of 0.2 Crab — a quite considerable value in the AGN flare detection.

If the 4 ponds are merged together to form a big pond, the sensitivity will increase, approximately 3–4 times better at the median energy of ≈ 3 TeV. If a layer of muon detectors are added under the water, based on the results of a simple simulation, the sensitivity will increase roughly 30% at the high energy band (>1 TeV). This preliminary estimation of the new detector configuration is shown in figure 8.

Nevertheless, more work on simulation and optimisation with the real detector configuration and measured environment parameters shall be continued, to give more reliable results about the detector performance.

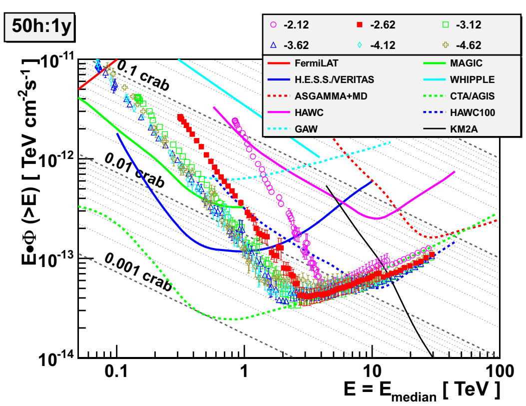

Figure 8: Preliminary estimation of the sensitivity of LHAASO-WCDA, configured in 1 big pond while a layer of muon detectors are added.

4 Conclusion

The LHAASO-WCDA detector have been conceptually designed basically, from the detector configuration, the water quality maintenance, to the calibration systems. Simulations show that the detector has a great performance in observing gamma ray sources, especially in detecting flare signals, quite competitive and complementary to next generation IACTs. As a R&D, A water Cherenkov prototype has been built in Beijing [6], and an engineering array of 9 cells constructed in Yang-Ba-Jing is running [9] now. Progress of the R&D work and further Monte Carlo simulations will offer more optimization and new idea in the detector design, finally come to a practically technical design report of the project by the mid next year.

Acknowledgment

The authors would like to express their gratitude once more to the Milagro Collaboration for the beneficial discussions on the detector design and simulations.

References

[1] Weeks, T. C., *et al*., Astrophys. J. **342** (1989) 379–395.
[2] Wagner, R., `http://www.mppmu.mpg.de/~rwagner/sources/`.
[3] Spiering, C., `arXiv:0804.1500v1 [astro-ph]`.
[4] Cao, Z. *et al*., for the LHAASO Collaboration, Proceedings of 31th ICRC (2009).
[5] Gao, B. *et al*., for the LHAASO Collaboration, Proceedings of 32th ICRC (2011).
[6] An, Q. *et al*., the LHAASO Collaboration, NIM **A 644** (2011) 11–17.
[7] Wu, H. R. *et al*., for the LHAASO Collaboration, Proceedings of 32th ICRC (2011).
[8] Yao, Z. G. *et al*., for the LHAASO Collaboration, Proceedings of 31th ICRC (2009).
[9] Chen, M. J. *et al*., for the LHAASO Collaboration, Proceedings of 32th ICRC (2011).